Physiological Measurement 38(1) (N16)

DOI: 10.1088/1361-6579/38/1/N16

iTrack: instrumented mobile electrooculography (EOG) eye-tracking in older adults and Parkinson's disease

Samuel Stuart, Aodhán Hickey, Brook Galna, Sue Lord, Lynn Rochester and Alan Godfrey

Institute of Neuroscience/Newcastle University Institute of Ageing, Newcastle University, UK

Correspondence to:

Dr Samuel Stuart

Clinical Ageing Research Unit
Campus for Ageing and Vitality
Newcastle upon Tyne
NE4 5PL
Tel: +44191 208 1242
Email: sam.stuart@newcastle.ac.uk

Word Count: Abstract: (300) 271
Article (Excluding abstract): (3,500) 3,495
Figures: 5
Tables: 4

Abstract

Detection of saccades (fast eye-movements) within raw mobile electrooculography (EOG) data involves complex algorithms which typically process data acquired during seated static tasks only. Processing of data during dynamic tasks such as walking is relatively rare and complex, particularly in older adults or people with Parkinson's disease (PD). Development of algorithms that can be easily implemented to detect saccades is required. This study aimed to develop an algorithm for the detection and measurement of saccades in EOG data during static (sitting) and dynamic (walking) tasks, in older adults and PD. Eye-tracking via mobile EOG and infra-red (IR) eye-tracker (with video) was performed with a group of older adults (n=10) and PD participants (n=10) (≥50 years). Horizontal saccades made between targets set 5°, 10° and 15° apart were first measured while seated. Horizontal saccades were then measured while a participant walked and executed a 40° turn left and right. The EOG algorithm was evaluated by comparing the number of correct saccade detections and agreement ($ICC_{2,1}$) between output from visual inspection of eye-tracker videos and IR eye-tracker. The EOG algorithm detected 75-92% of saccades compared to video inspection and IR output during static testing, with fair to excellent agreement ($ICC_{2,1}$ .49 to .93). However, during walking EOG saccade detection reduced to 42-88% compared to video inspection or IR output, with poor to excellent ($ICC_{2,1}$ .13 to .88) agreement between methodologies. The algorithm was robust during seated testing but less so during walking, which was likely due to increased measurement and analysis error with a dynamic task. Future studies may consider a combination of EOG and IR for comprehensive measurement.

Key Terms: Electrooculography, eye-tracking, Parkinson's disease, saccades, algorithm

I. INTRODUCTION

Monitoring eye-movements with non-invasive recording devices is becoming increasingly popular, likely due to the close relationship between eye-movements and cognition [1]. Eye-movement measurement is an important part of patient neurological examinations [2], particularly saccadic (fast) and fixation movements. Visual and cognitive impairments are common in Parkinson's disease (PD) compared to healthy older adults [3, 4], and are associated with reduced mobility and falls [7, 8]. Visual and cognitive processes can be measured during dynamic tasks (e.g. walking) by tracking eye-movements [1, 6]. Eye-movement abnormalities in PD [5] relate to impairment of particular brain areas (i.e. the basal ganglia and frontal cortex) and cognitive processes (i.e. attention, visuo-spatial ability etc.). Understanding eye-movement abnormalities in PD compared to older adults during walking will inform appropriate intervention application and development.

Eye-tracking technology has progressed from large/expensive/static devices (e.g. EyeLink 1000, Tobii Pro TX300 etc.) to mobile devices capable of real-time eye-tracking during functional tasks (e.g. walking/gait), such as electrooculography (EOG). EOG is an eye-tracking technique based on measurement of corneo-retinal standing potentials that exist between the front and back of the eye, due to the higher metabolic rate of the retina compared to the cornea [2]. The eye acts as a dipole orientated from retina to cornea. EOG is reliant upon the steady difference in potential (range ~0.4-1.0mV) that exists between the retina and cornea, producing an electrical field [7]. The bi-potential electrical signal can be recorded from the skin near the eyes. Eye-movements change potentials generated and provide a signal with which to measure saccades (Fig. 1) [8]. EOG is usually recorded in voltage via two bipolar electrodes, which are placed either side of the eyes (on the lateral canthus) to measure horizontal eye-movements. Some studies also record vertical eye-movements by placing a second set of electrodes above and below one eye. However, vertical eye-movements are difficult to record due to substantial impact on the signal by blinks and facial muscle movement, which can lead to problems differentiating between saccades and other artefacts. Eye-movement can be inferred from voltage signals obtained from EOG system with previously reported accuracy of ±1.5-2° [2, 9].

EOG is often referred to as an 'ideal eye-tracking system', primarily due to its large sampling frequency (200-1000Hz), non-invasive methods and relationship between recorded voltages and angular displacement of the eyes [8]. There are however problems using EOG, particularly during dynamic tasks (e.g. walking). For example; visual field data is not obtained from EOG, as unlike video-based eye-tracking there is no method for recording the scene/environment. Other issues such as signal drift have also been reported [10], which would require re-calibration during long trials [11]. Due to limitations new eye-tracking technologies (i.e. mobile infra-red (IR) eye trackers) have not only been developed, but seem to be the predominant method used in research studies. However EOG remains useful due to its high sampling rates, but data processing is difficult without in-depth understanding of EOG signal from eye-movement. Therefore to derive saccades and fixations from EOG an algorithm is required. Previous studies [2, 10, 12, 13] have developed complex algorithms during static seated tasks. However EOG eye-movement classification remains challenging, particularly during dynamic tasks due to increased subject movement [12]. Hence, there are currently no published algorithms to detect eye-movements in EOG signal during dynamic tasks, although algorithms developed within static conditions may be applicable. Development and evaluation of easily implementable, yet reliable EOG algorithms for use in both static and dynamic tasks is required.

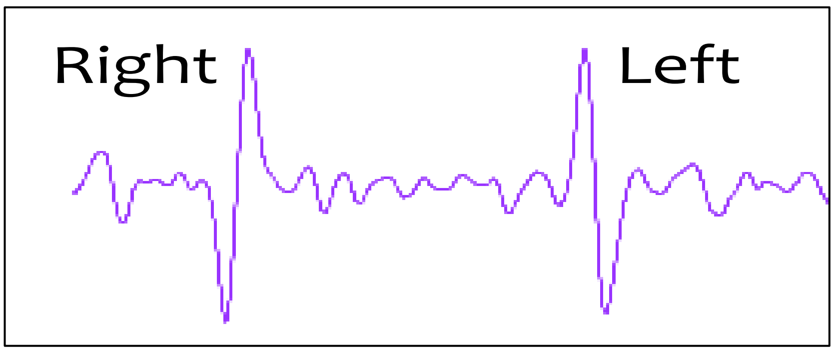

Fig. 1: A standard electrooculography (EOG) trace during one of the static calibration tasks (horizontal eye-movements).

- Left: the cornea approaches the electrode near the outer canthus of the left eye, resulting in a positive to negative change in the recorded potential.
- Right: the cornea approaches the electrode near the inner canthus of the left eye, resulting in a negative to positive change in the recorded potential.

Aims:

1. Develop an algorithm to detect saccades within EOG data during static (sitting) and dynamic (walking) testing.
2. Compare EOG algorithm output to video-based visual inspection and a previously validated infra-red mobile eye tracker algorithm [14].

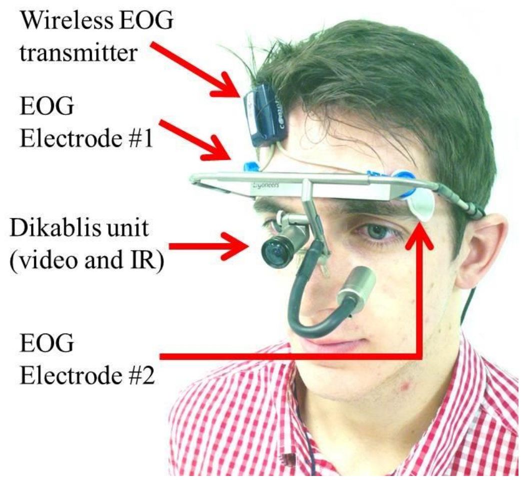

Fig. 2: System set up. Head mounted Dikablis unit (IR and video camera) and EOG electrodes (×2, left/right temporal regions)

II. METHODS

Participants

Data were collected within an ongoing study 'Vision and Gait in Parkinson's disease' at Newcastle University and had ethical approval (Reference; 13/NE/0128) [15]. Written informed consent was gained prior to testing. This study involved recording eye-movements while sitting and walking while turning in people with PD and healthy older adult controls (HC). Data from twenty participants were chosen at random from the larger study to be analysed.

Equipment

<u>EOG</u>: Wireless mobile EOG (Zerowire, Aurion, Italy) recorded horizontal saccades (1000Hz). Electrodes (~4mm) were placed bi-temporally as close to the (left and right) lateral canthus as possible without blocking the participants vision (Fig. 2).

<u>IR</u>: Head-mounted Dikablis mobile eye-tracker (Ergoneers, GmbH, Germany) also recorded participant saccades simultaneously (50Hz). Participants left pupil was tracked by means of IR illumination and provided gaze co-ordinates (x, y). This device (including video) was automatically synchronized to EOG by a 3D motion analysis system (Vicon, Oxford, UK).

<u>Video</u>: IR used a dual camera system, with one monocular infra-red eye camera and one fish-eye field-camera (50Hz). IR video was calibrated prior to EOG calibration via a four point calibration method [16], which overlaid video output from both of the cameras with a cross-hair provided on the video to represent pupil location. Co-ordinate data was derived from the cross-hair position and used to derive eye-movements.

Procedure

1) Static: Seated Eye-Movement (Calibration)

EOG was calibrated for each participant prior to walking trials. Participants were seated ~6m from a wall and a marker was placed straight in front of them. We asked participants to blink for a period of 30 seconds (s) in time with a 60bpm metronome. Next, participants moved their eyes between two markers placed at set distances (5°, 10°, 15°), again in time with the metronome for 30s [16]. A maximum distance of 15° was used as most naturally occurring saccades occur within this threshold [17]. Horizontal eye-movements (5°, 10°, 15°) were recorded via EOG (1000Hz), video and IR (both 50Hz) simultaneously during this procedure and later compared.

2) Dynamic: Walking Trials

Participants walked straight for 2.5m and then made a right or left 40° turn once they had walked through a doorway. Tasks were repeated three times and the average of the six trials were calculated. EOG, IR and video data were recorded during these walks from which saccades could be measured [15].

Feature Selection and Evaluation

<u>Video Inspection:</u> Videos were analysed similar to previous work [14]. All IR videos (eye/field-camera) for each participant (n=20) during static and dynamic trials were visually inspected by a single examiner (AH) frame-by-frame, in order to compare algorithm results (180 videos in total). Video inspection of the dynamic tasks was calibrated by the examiner viewing the static seated videos and measuring participant 5° eye-movements prior to the walking videos in order to provide a reference for saccade distance (i.e. ≥5°).

Number of saccades detected via video inspection during static and dynamic tasks was recorded and compared to number measured via EOG algorithm. EOG algorithm saccade detection performance was also compared to our previously validated IR algorithm [14]. Finally, more specific characteristics of the horizontal eye-movements (e.g. velocity and distance) recorded by EOG were compared to IR.

III. EOG signal processing Algorithm

An EOG algorithm was developed to analyse data collected during static and dynamic tasks. The algorithm was based upon a previously developed EOG algorithm used within seated testing [13] and our previous IR algorithm used within walking [14]. These studies guided algorithm development, which we evaluated within both static and dynamic conditions. Full algorithm representation is presented in Fig. 3.

STAGE 1: pre-processing

a) Baseline offset removal

Mean EOG signal was calculated and then removed in order to account for baseline offset.

b) Filtering

EOG signal was filtered to remove noise introduced by artifacts, such as facial muscle activity, using a band-pass filter (0.1-20Hz). This filter was chosen to preserve the edge steepness of the saccades, retain signal amplitudes and not introduce any artificial signal changes [18].

STAGE 2: Detection of EOG signal characteristics

a) Create a conversion factor

Eye-movements are typically measured and reported in degrees but EOG provides data in voltage (Table 1). Therefore, to determine the ratio of volts to degrees of eye-movement it is necessary to construct a conversion factor (i.e. amount of volts when the eyes move to set-distance targets; -15°, -10°, -5°, 0°, 5°, 10°, 15° [13].

Table 1 - Conversion Factor Example From One Participants Data

Known Saccade Distance	Mean Voltage (mV)	Conversion Factor (volts/°)
5°	0.0075	0.0015
10°	0.015	0.0015
15°	0.019	0.0013
Conversion value (mean of 5°, 10°, 15°)		0.0014

A conversion factor was calculated for each participant before further processing. The conversion factor is the average voltage generated at each set-distance of eye-movement divided by the known degree value (i.e. 5°, 10°, and 15°). Final conversion value is the average of the three conversion factors. Table 1 shows an example from one participants data, which provides reference for voltage to degrees of eye-movement (e.g. 1° = 0.0014mV).

b) Peak detection

After filtering, peak detection was used to locate the peaks (positive and negative) of eye-movement within EOG signal (Fig. 1.). These peaks were identified using a minimum peak voltage threshold identified within the calibration procedure (e.g. 5° = peaks > or < 0.0075mV). The algorithm then classified the detected peaks as either left or right eye-movements based on whether a positive or negative peak occurred first or second, within a particular duration (100ms). Velocity and acceleration thresholds were then used to further classify eye-movements.

STAGE 3: Detection of EOG visual events

a) Velocity and Acceleration based thresholds

Similar to a previous EOG algorithm for static tasks [13], velocity (1) and acceleration (2) values (*V* and *A*, respectively) were used to discriminate between different types of eye-movements. Moment-to-moment change (*D*) in EOG signal (*X*) was calculated and divided by change (*D*) in time (*T*) [13, 14].

Thresholds were adaptable (i.e. could be changed depending upon the task), but within this study they were fixed to the same settings as below during both static and dynamic tasks.

$$V = D(X)/D(T) \times \text{Sample Frequency} \quad (1)$$

$$A = D^2(V)/D(T) \times \text{Sample Frequency} \quad (2)$$

b) Saccade Detection

A velocity-threshold of ≥240°/s (~5° eye-movement) and acceleration-threshold of ≥3,000°/s² were used to detect saccades, which were also screened for duration set at ≤100ms [19]. Duration screening was used to eliminate inclusion of facial muscle activity, blinks or smooth pursuit eye-movements.

c) Fixation Detection

Once saccades had been detected, fixations were classified as data which was not a saccade or artefact. In order to prevent other artefacts being picked up as a fixation, each fixation had to be ≥100ms in duration, as well as meeting non-saccade criteria (i.e. <240°/s velocity and <3000°/s² acceleration). There is no consensus for fixation duration criteria (with some as short as 50ms), but most studies use a minimum duration of 100-200ms [20, 21]. Fixation duration criteria are based on an estimation of the minimum time required for appropriate visual intake [19].

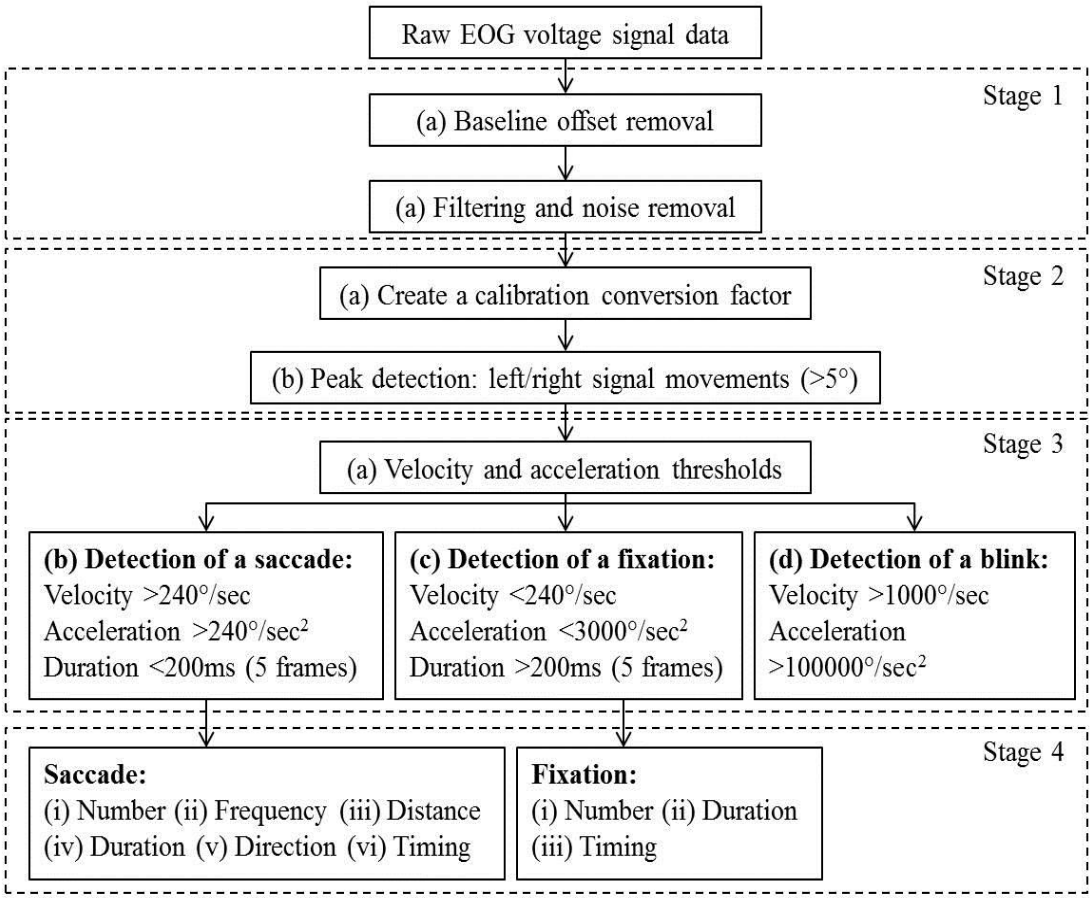

Fig. 3: Flow chart of electrooculography (EOG) algorithm

d) Blink and artefact removal

Raw EOG data was further filtered using the same threshold criteria for blinks and other artefacts as used within our previous IR algorithm [14], as horizontal signal from blinks closely resembles that of eye-movements [22, 23]. The filtering involved the removal of data which met criteria as being an un-physiological eye-movement (i.e. a human would be unable to move their eye at a certain speed) and therefore were most likely a blink. Removal was based upon thresholding the raw signal, velocities and accelerations of the detected peaks [24, 25]. If an eye-movement had a velocity of >1,000°/s or an acceleration of >100,000°/s^2, these data represented blinks/artefacts and were removed.

STAGE 4: Feature Extraction

The final algorithm stage was to calculate and output various saccade and fixation characteristics. Characteristics included saccade number, frequency, distance, duration, direction (horizontal) and timing. Fixation characteristics included number, duration and timing.

IV. Data Analysis

The EOG algorithm was implemented using MATLAB® (2012a, Mathworks, Natick, MA, USA). EOG was compared to video and our previously validated IR algorithm [14]. Between group (PD, HC) comparison was not performed as this was not the focus of the study. Saccade detection (horizontal only) was evaluated during static (seated; 5°, 10° and 15°) and dynamic (walking) tasks. Detection performance was performed with respect to the following criteria:

- Correct detection: Algorithm saccade detection was marked as correct if it was found in the corresponding video or IR algorithm output.

- Undetected: Algorithm saccade detection was marked as undetected if the saccade was found in the corresponding video or IR algorithm output, but not in the algorithm output.

- Spurious: Algorithm saccade detection was marked as spurious if it was in the EOG algorithm output but not in the corresponding video or IR algorithm output.

Average values obtained for several saccade characteristics (i.e. number, duration, peak velocity, distance) were tabulated. Intra-class correlations ($ICC_{2,1}$) were quantified using SPSS V21 (SPSS Inc., IL) to assess the absolute agreement between methodologies (EOG, video inspection and IR). $ICC_{2,1}$ was interpreted as; poor <0.39, fair >0.40-0.59, good 0.60-0.75 and excellent >0.75 [26]. Histogram comparisons of overall saccade measurements (number, velocity, distance and duration) from each method (video, IR, EOG) are also presented.

V. Results

Static: Eye-Movement Calibration

Table 2 shows that compared to video, a similar number of horizontal saccades (5°, 10°, 15°) were detected within EOG and IR output during static calibration. Saccade peak velocity and distance tended to increase with increasing target distance for both EOG and IR, and within both groups (HC and PD). Table 3 demonstrates saccade detection performance of the EOG algorithm compared to video inspection and IR. Results showed that during static testing EOG detected 86-92% of saccades found within video inspection and 75-83% of saccades detected by IR. On average there were more spurious detections than undetected (Undetected; video: 9%, IR: 14% and Spurious; video: 0.4%, IR: 7%). Agreement between output from video and the two eye-tracking systems (EOG, IR) during static eye-movement calibration is shown in Table 4 and graphically depicted in Fig. 4. Results indicated that the EOG algorithm can detect saccades (number) with fair ($ICC_{2,1}$ .49) to excellent ($ICC_{2,1}$ .93) agreement to video inspection and IR for both PD and HC groups, with better agreement with video inspection. However, the majority of the saccade number results showed good to excellent agreement for both groups. There was inconsistent agreement between EOG and IR output within either group for saccade duration, peak velocity or distance ($ICC_{2,1}$ range; .02 to .40).

Dynamic: Walking Trials

Results for video inspection and EOG and IR algorithm output during walking trials (LT, RT) are displayed in Table 2 and 3. Overall EOG detected approximately 76% of the saccades detected via video inspection, and 52% of the saccades detected via IR, which was lower than static testing. There were also higher levels of undetected and spurious saccade detections within the EOG data during dynamic testing compared to static (Undetected; video: 20% and IR: 27% and Spurious; video: 5% and IR: 23%).

Agreement results shown in Table 4 and graphically depicted in Fig. 5, indicated that the EOG algorithm detected saccades while walking with good to excellent ($ICC_{2,1}$ .60 to .88) agreement to video, and poor to fair agreement to IR ($ICC_{2,1}$ .13 to .55). However, agreement between EOG and video and IR was reduced while walking compared to the static testing (e.g. $ICC_{2,1}$ .76 during calibration but .58 when walking, Table 4). Other saccade characteristics of duration, peak velocity and distance had variable agreement during walking ($ICC_{2,1}$ range; .06 to .50).

TABLE 2 - AVERAGE SACCADE CHARACTERISTICS

Group		Video (50Hz)	IR (50 Hz)				EOG (1000 Hz)			
		Number	Number	Duration (sec)	Peak Velocity (°/sec)	Distance (°)	Number	Duration (sec)	Peak Velocity (°/sec)	Distance (°)
HC (n=10)	5°	24 (4)	23 (8)	0.03 (0.01)	289.6 (47.1)	5.7 (0.7)	22 (4)	0.05 (0.01)	456.2 (33.9)	6.6 (1.4)
	10°	23 (3)	22 (5)	0.03 (0.01)	451.9 (114.8)	9.0 (2.5)	21 (3)	0.05 (0.00)	634.8 (124.3)	10.8 (2.4)
	15°	29 (12)	31 (17)	0.04 (0.01)	583.2 (103.8)	10.4 (1.8)	25 (10)	0.06 (0.01)	572.3 (98.8)	11.0 (2.1)
	LT	4 (0)	3 (1)	0.03 (0.00)	428.0 (20.9)	10.8 (0.9)	3 (0)	0.05 (0.01)	469.2 (7.72)	8.2 (1.8)
	RT	3 (0)	3 (0)	0.03 (0.01)	432.4 (53.2)	10.6 (1.4)	3 (0)	0.05 (0.01)	427.0 (15.74)	6.4 (0.7)
PD (n=10)	5°	29 (6)	27 (5)	0.03 (0.01)	314.7 (126.0)	5.7 (1.2)	28 (7)	0.05 (0.00)	521.6 (62.3)	6.6 (2.5)
	10°	32 (9)	31 (10)	0.03 (0.01)	398.0 (120.3)	7.9 (2.1)	29 (10)	0.05 (0.00)	606.1 (160.3)	9.7 (2.8)
	15°	25 (6)	30 (8)	0.03 (0.01)	462.8 (144.4)	9.0 (2.3)	23 (5)	0.05 (0.00)	612.3 (116.6)	10.7 (2.7)
	LT	3 (0)	2 (0)	0.03 (0.00)	400.8 (43.5)	10.3 (2.5)	2 (0)	0.05 (0.01)	510.3 (45.4)	8.1 (1.4)
	RT	3 (0)	3 (0)	0.03 (0.00)	382.3 (11.9)	9.5 (0.5)	2 (1)	0.05 (0.01)	490.0 (75.3)	9.5 (0.9)

[RT = Right turns, LT = Left turns, Mean (SD) reported for horizontal saccades only]

TABLE 3 - OVERALL EOG ALGORTIHM SACCADE (NUMBER) DETECTION PERFORMANCE

		Video (50Hz) vs EOG (1000Hz)					IR (50 Hz) vs EOG (1000Hz)				
		Static			Dynamic		Static			Dynamic	
Group		5°	10°	15°	LT	RT	5°	10°	15°	LT	RT
HC (n=10)	Correct Detection: n (%)	221 (91.7)	212 (91.8)	247 (86.4)	98 (80.2)	85 (88.0)	225 (78.7)	216 (83.1)	266 (76.9)	61 (49.3)	50 (58.0)
	Undetected: n (%)	19 (7.9)	19 (8.2)	38 (13.3)	19 (15.5)	9 (9.3)	32 (11.2)	24 (9.2)	71 (20.5)	33 (25.6)	16 (16.1)
	Spurious: n (%)	1 (0.4)	0 (0.0)	1 (0.3)	5 (4.3)	3 (3.3)	29 (10.1)	29 (7.7)	9 (2.6)	31 (25.1)	30 (31.9)
PD (n=10)	Correct Detection: n (%)	272 (91.9)	291 (92.4)	225 (88.9)	58 (75.9)	58 (58.0)	242 (82.3)	272 (81.4)	233 (74.9)	48 (58.8)	42 (42.2)
	Undetected: n (%)	21 (7.1)	24 (7.6)	26 (10.3)	18 (21.4)	35 (34.1)	19 (6.5)	38 (11.4)	74 (23.8)	24 (27.7)	41 (37.6)
	Spurious: n (%)	3 (1.0)	0 (0.0)	2 (0.8)	2 (2.7)	9 (8.0)	33 (11.2)	24 (7.2)	4 (1.3)	11 (13.5)	24 (20.2)

[Horizontal saccade detection performance, n = sum of saccades made over all trials in all participants]

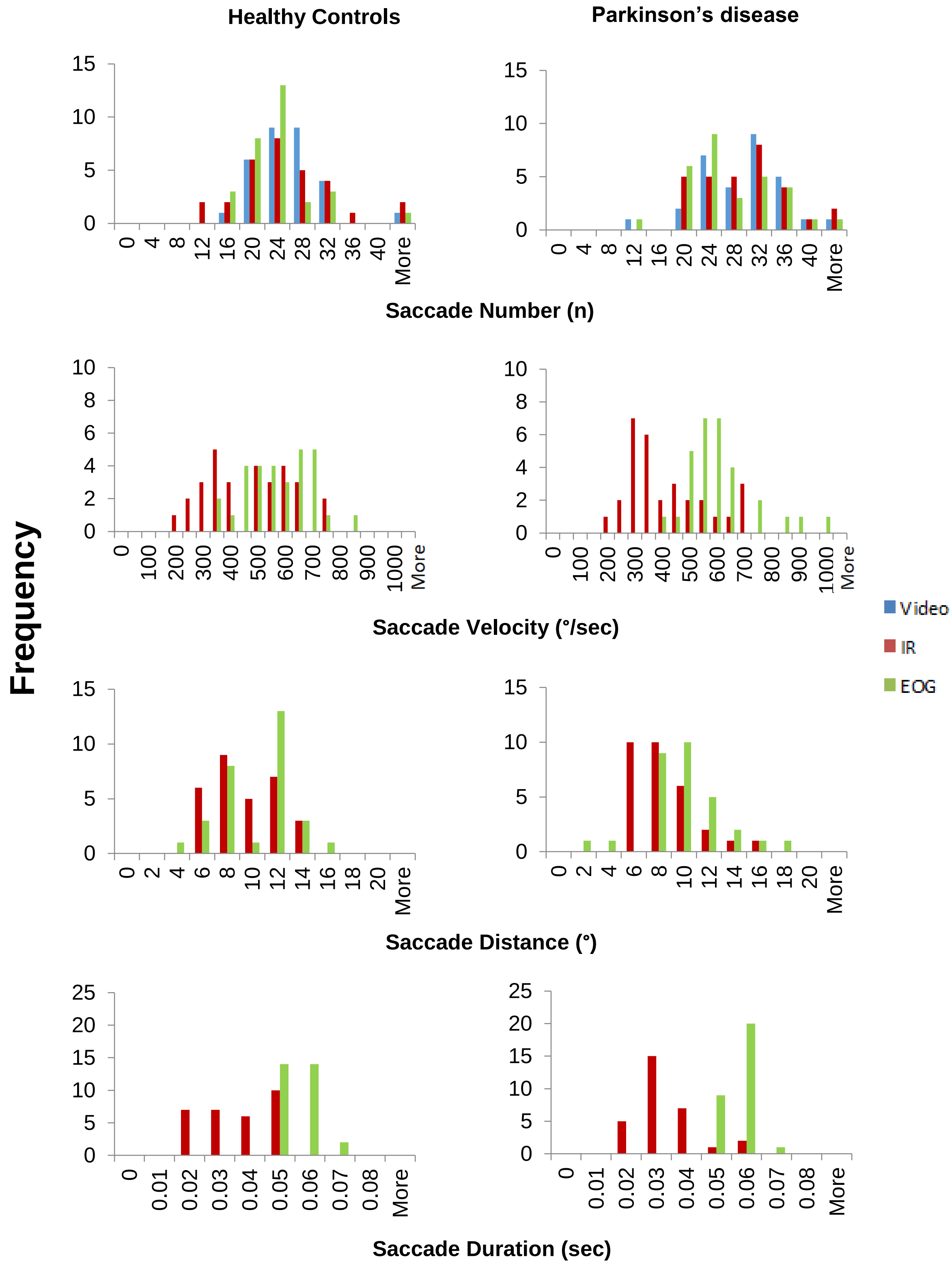

Fig. 4: Histogram comparisons across methods for static saccade measurements

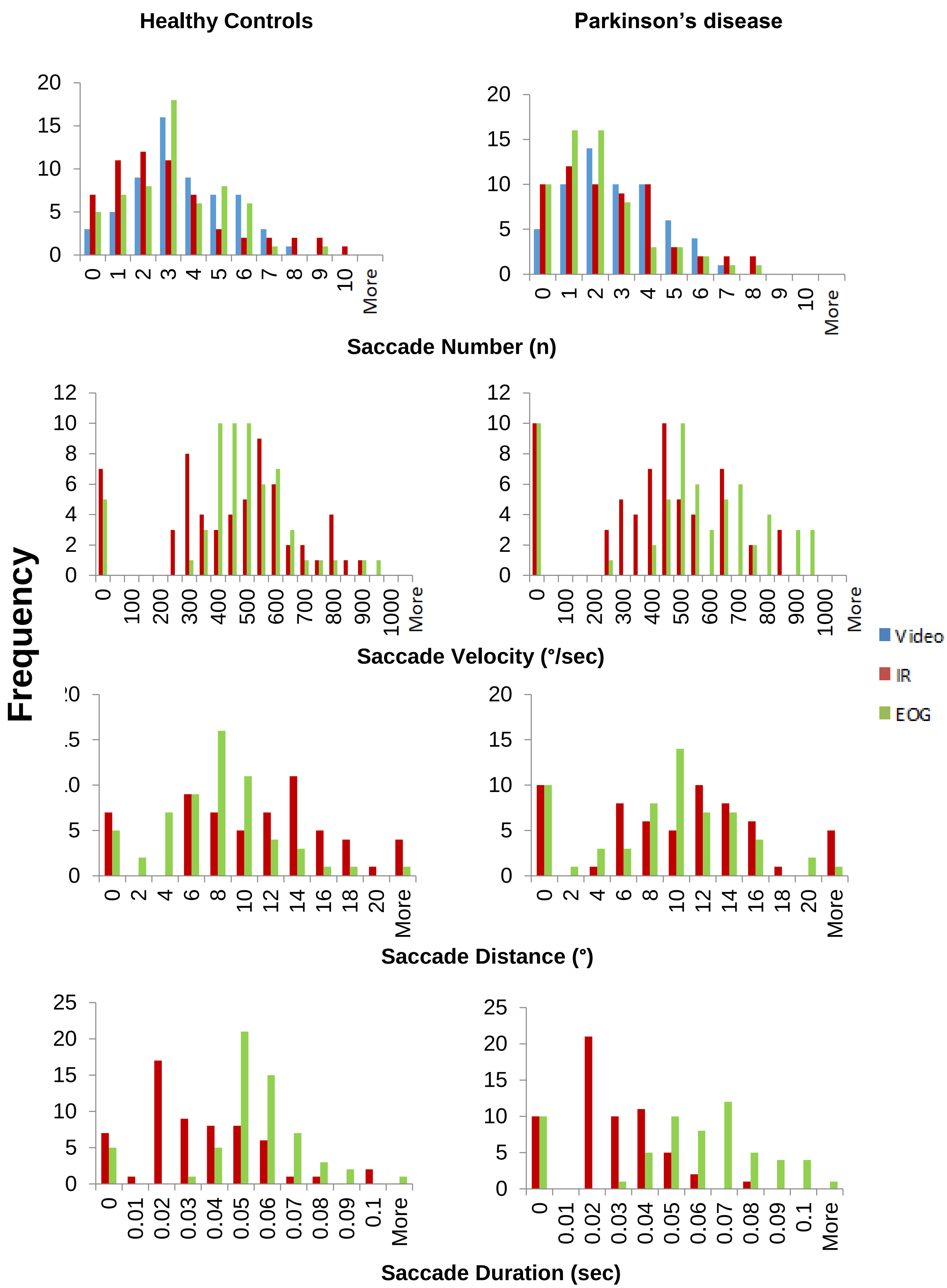

Fig. 5: Histogram comparisons across methods for dynamic saccade measurements

TABLE 4 - ALGORITHM & SYSTEM AGREEMENT: ICC$_{2,1}$

Group		EOG vs Video vs IR	EOG vs Video	EOG vs IR			
		Number	Number	Number	Duration (sec)	Peak Velocity (°/sec)	Distance (°)
HC (n=10)	5°	0.76	0.87	0.59	0.02	0.29	0.41
	10°	0.74	0.87	0.57	0.02	0.26	0.37
	15°	0.73	0.87	0.56	0.07	0.18	0.37
	LT	0.58	0.82	0.30	0.14	0.08	0.23
	RT	0.67	0.88	0.45	0.35	0.49	0.24
PD (n=10)	5°	0.68	0.92	0.49	0.10	0.36	0.35
	10°	0.69	0.92	0.51	0.16	0.28	0.27
	15°	0.71	0.93	0.53	0.03	0.40	0.34
	LT	0.73	0.75	0.55	0.46	0.50	0.35
	RT	0.43	0.60	0.13	0.20	0.18	0.06

[RT = Right turns, LT = Left turns, Horizontal saccade characteristics displayed]

VI. DISCUSSION

This study developed and evaluated an algorithm to detect saccades within EOG data collected during static and dynamic testing in older adults and people with PD. To our knowledge no previous studies have developed or tested EOG algorithms within dynamic tasks such as walking, instead algorithms developed within static conditions are often used. Similar to previous work [14, 27], we compared the developed algorithm to frame-by-frame video inspection and also compared to a previously validated IR algorithm [14].

Robust evaluation of automated algorithms for the analysis of eye-movement (saccade) data is vital to ensure confidence in outputs on which clinical decisions may be made. Similar to our previous IR algorithm [14] and a previous static EOG algorithm [13], a velocity-based method was used to detect horizontal saccades within an EOG signal. Although velocity-based algorithms may not have the accuracy of dispersion-based approaches [20, 21] we believe that the easy implementation [21, 28] of our developed velocity-based algorithm gives it an advantage, as it allows implementation by those with limited algorithmic experience (e.g. clinicians or novice researchers). However this study suggests that developed EOG algorithms which are relatively robust within static testing may not be as consistent within dynamic testing. Results highlight the need for further development of EOG algorithms or methodologies to derive saccadic data during dynamic tasks.

EOG algorithm robustness

To determine robustness, participants performed two separate procedures and data were analysed using the same fixed algorithm settings for both procedures. The two separate procedures were: (i) static testing, eye-movements to set distances while sitting, and (ii) dynamic testing, several repeated walking trials (left and right turns).

i. Static testing: Saccades to set distances during sitting

To calibrate the EOG system all participants made eye-movements (saccades) between two horizontal targets placed 5°, 10° and 15° apart, which derived a conversion factor and completed Stages 1-2 of the algorithm. After initial calibration the same eye-movement data (5°, 10° and 15°) was used to assess the algorithm for detection and measurement of saccades in EOG data (algorithm Stage 3 onwards). Under these conditions, the algorithm proved relatively robust at detecting saccades (number) during static testing. It detected 75-92% of the saccades detected via video inspection or IR, with primarily excellent agreement with video inspection (Table 4). However, agreement between EOG and IR was not as consistent, and reduced for saccade number, duration, peak velocity and distance.

Inconsistency between EOG and IR for saccade detection and measurement, particularly characteristics of velocity and distance, likely related to device sampling frequencies (i.e. EOG 1000Hz vs IR 50Hz). The EOGs larger sampling frequency meant that more frequent eye-movement data was collected and therefore saccade measurement may have been more accurate [19, 29], hence not similar to data collected from IR. Despite this, output from both systems/algorithms demonstrated increased saccade peak velocity and distance with increased target distance (5°, 10° and 15°, Table 2).

ii. Dynamic testing: Horizontal saccades during walking

The main advantage of this study is the novel comparison of EOG with video inspection and IR during walking. While walking mobile EOG detected ~63% of the saccades detected via video or IR methodologies, with greater undetected (average of 30%) and spurious (average of 11%) saccades than static testing. Similarly, agreement between EOG and video inspection, as well as IR for saccade number was reduced compared to static testing. Agreement ranged from poor to excellent for saccade number for both groups (Table 4). This demonstrated that the developed EOG algorithm was capable of detecting saccades during walking but with reduced consistency compared to video or IR.

Reduction in saccade detection in comparison to video inspection and IR when walking likely related to increased error caused by the dynamic task. For example; walking increases number of artefacts which could infiltrate EOG signals (e.g. facial muscle activity). Similarly, the EOG device only measured horizontal saccades (largely due to difficulties with vertical EOG signal analysis), whereas video inspection and IR can detect saccades in all directions which may have led to inconsistencies between devices. To capture multi-directional mobile EOG signal future studies may consider simultaneous measurement of vertical mobile EOG signal, but must ensure robust data collection and analysis (i.e. blink detection and EOG electrode placement may be an issue if concurrently recording IR; Fig. 2) before reporting results.

Alternatively, video inspection or IR may have also missed saccades that the EOG system captured (spurious saccades). For example; issues such as incorrect or absent pupil tracking caused by eye-lashes or eye-lids may be more frequent when walking. Such issues would lead to saccades not being detected by IR [30], but would not affect EOG. Similarly, the majority of the participants (HC = 8/10, PD = 6/10) wore vision correction (i.e. glasses or contact lenses). Vision correction can interfere with IR pupil tracking due to infra-red refraction [19, 30, 31], which worsens during dynamic movement. This may be one explanation as to the lower saccade detection agreement and increased spurious saccades during walking compared to during static testing.

Despite similar average values for saccade duration, velocity and distance measured via EOG and IR, agreement for these features during static and dynamic testing was inconsistent. It is likely that difference in device sampling frequency (1000Hz vs 50Hz) led to EOG algorithm output providing more accurate data compared to IR output [19, 29]. Head-mounted IR eye-trackers have a mobility-resolution trade-off (i.e. more mobile devices tend to have lower sampling frequency than that of static devices; 50Hz compared to 1000Hz). The lower resolution means that researchers investigating saccades characteristics are limited (i.e. devices ≥50Hz are capable of detecting a saccade accurately but not specific characteristic; peak velocity, duration etc.). Until mobile IR devices with high sampling frequency (>200Hz [6]) are available, a combination of EOG and IR may be useful during dynamic tasks to provide comprehensive measurement.

Limitations

One limitation was that a velocity threshold of ≥240°/sec (~5° distance) may rule out smaller but detectable saccades within EOG signal [32]. This threshold was used for comparison to the previously validated mobile eye-tracker algorithm [14], as during walking other artefacts such as vestibular ocular-reflex may infiltrate eye-movement data. The ≥240°/sec velocity-threshold was chosen to avoid such infiltration. However, this threshold can be adapted depending upon the task being undertaken (i.e. lower threshold for static tasks) and could be changed for future studies.

VII. Conclusion

We developed and assessed an algorithm for saccade detection and measurement in EOG signal obtained from static and dynamic tasks in older adults and people with PD. The algorithm can detect saccades in EOG data and agreed well with video inspection and IR algorithm output during static testing. However agreement reduced during dynamic testing, as this introduces numerous sources of error. Future studies should consider a combination of EOG and IR for comprehensive measurement.

Acknowledgment

The authors acknowledge Henry King (MRes student) for his assistance with data collection. This research is supported by the National Institute for Health Research (NIHR) Newcastle Biomedical Research Unit (BRU) and Centre (BRC) based at Newcastle upon Tyne Hospitals NHS Foundation Trust and Newcastle University. The research was also supported by NIHR Newcastle CRF Infrastructure funding. The views expressed are solely those of the authors.

References

1. Stuart, S., et al., *Gait in Parkinson's disease: A visuo-cognitive challenge.* Neuroscience & Biobehavioral Reviews, 2016. **62**: p. 76-88.
2. Liu, C.C., et al., *Quantitative analysis on electrooculography (EOG) for neurodegenerative disease.* AIP Conference Proceedings, 2007. **953**(1): p. 246-253.
3. Weil, R.S., et al., *Visual dysfunction in Parkinson's disease.* Brain, 2016.
4. Yarnall, A.J., et al., *Characterizing mild cognitive impairment in incident Parkinson disease: The ICICLE-PD Study.* Neurology, 2014. **82**(4): p. 308-316.
5. Armstrong, R.A., *Visual symptoms in Parkinson's disease*. Parkinsons Dis, 2011. **1**(2011): p. 1-9.
6. Stuart, S., et al., *The measurement of visual sampling during real-world activity in Parkinson's disease and healthy controls: A structured literature review*. J Neurosci Methods, 2014. **222**: p. 175-88.
7. Bannerman, R.L., M. Milders, and A. Sahraie, *Attentional bias to brief threat-related faces revealed by saccadic eye movements.* Emotion, 2010. **10**(5): p. 733-738.
8. Heide, W., et al., *Electrooculography: technical standards and applications. The International Federation of Clinical Neurophysiology.* Electroencephalogr Clin Neurophysiol Suppl, 1999. **52**: p. 223-40.
9. Young, L. and D. Sheena, *Survey of eye movement recording methods.* Behavior Research Methods & Instrumentation, 1975. **7**(5): p. 397-429.
10. Pettersson, K., et al., *Algorithm for automatic analysis of electro-oculographic data.* BioMedical Engineering OnLine, 2013. **12**: p. 110-110.
11. Keegan, J., E. Burke, and J. Condron, *An electrooculogram-based binary saccade sequence classification (BSSC) technique for augmentative communication and control*, in *Engineering in Medicine and Biology Society. EMBC 2009. Annual International Conference of the IEEE*. 2009, IEEE: Minneapolis, Minnesota p. 2604-2607.
12. Cona, F., et al., *An improved algorithm for the automatic detection and characterization of slow eye movements.* Med Eng Phys, 2014. **36**(7): p. 954-61.
13. Vidal, M., A. Bulling, and H. Gellersen, *Analysing EOG Signal Features for the Discrimination of Eye Movements withWearable Devices*, in *PETMEI'11*. 2011: Beijing, China. p. 15-20.
14. Stuart, S., et al., *Quantifying Saccades While Walking: Validity of a Novel Velocity-Based Algorithm for Mobile Eye Tracking*, in *Engineering in Medicine and Biology Society, (EMBC) 2014. 36th Annual International Conference of the IEEE*. 2014, IEEE: Chicago, Illinois, USA. p. 5739 - 5742.
15. Stuart, S., et al., *A protocol to examine vision and gait in Parkinson's disease: impact of cognition and response to visual cues [version 2; referees: 2 approved].* F1000Research, 2016. **4**: p. 1379.
16. Stuart, S., et al., *Accuracy and re-test reliability of mobile eye-tracking in Parkinson's disease and older adults.* Medical Engineering and Physics, 2016. **38**(3): p. 308–315.
17. Bahill, A.T., D. Adler, and L. Stark, *Most naturally occurring human saccades have magnitudes of 15 degrees or less.* Invest Ophthalmol, 1975. **14**(6): p. 468-9.
18. Bulling, A. and D. Roggen, *Recognition of Visual Memory Recall Processes Using Eye Movement Analysis*, in *UbiComp'11*. 2011: Beijing, China.

19. Holmqvist, K. and M. Nystrom, *Eye tracking: A comprehensive guide to methods and measures*. 2011, Oxford, UK: Oxford University Press.
20. Nystrom, M. and K. Holmqvist, *An adaptive algorithm for fixation, saccade, and glissade detection in eyetracking data.* Behav Res Methods, 2010. **42**(1): p. 188-204.
21. Salvucci, D.D. and J.H. Goldberg, *Identifying Fixations and Saccades in Eye-Tracking Protocols*, in *Eye Tracking Research & Applications Symposium*. 2000: Palm Beach Gardens, FL, USA. p. 71-78.
22. Kong, X. and G. Wilson, *A new EOG-based eyeblink detection algorithm.* Behavior Research Methods, Instruments, & Computers, 1998. **30**(4): p. 713-719.
23. Nakanishi, M., et al., *Online voluntary eye blink detection method using electrooculogram.* Nonlinear Theory and Its Applications, 2012 International Symposium on, 2012: p. 114-117.
24. Reddy, M.S., et al. *Analysis of EOG signals using wavelet transform for detecting eye blinks*. in *Wireless Communications and Signal Processing (WCSP), 2010 International Conference on*. 2010.
25. Ebrahim, P., W. Stolzmann, and Y. Bin. *Eye Movement Detection for Assessing Driver Drowsiness by Electrooculography*. in *Systems, Man, and Cybernetics (SMC), 2013 IEEE International Conference on*. 2013.
26. Field, A., *Discovering statistics using IBM SPSS statistics*. 4th ed. 2013, London, UK: Sage. 915.
27. Pedrotti, M., et al., *A data-driven algorithm for offline pupil signal preprocessing and eyeblink detection in low-speed eye-tracking protocols.* Behav Res Methods, 2011. **43**(2): p. 372-83.
28. Salvucci, D.D. and J.R. Anderson, *Automated Eye-Movement Protocol Analysis.* HUMAN-COMPUTER INTERACTION, 2001. **16**: p. 39–86.
29. Andersson, R., M. Nyström, and K. Holmqvist, *Sampling frequency and eye-tracking measures: how speed affects durations, latencies, and more.* Journal of Eye Movement Research, 2010. **3**(3): p. 1-12.
30. Nystrom, M., et al., *The influence of calibration method and eye physiology on eyetracking data quality.* Behav Res Methods, 2013. **45**(1): p. 272-88.
31. Duchowski, A.T., *Eye Tracking Methodology: Theory and Practice*. 2nd ed. 2007, London: Springer.
32. Galna, B., et al., *Visual sampling during walking in people with Parkinson's disease and the influence of environment and dual-task.* Brain Res, 2012. **1473**: p. 35-43.